Superpixel-based C-SVC for Brain Tissue Classification in MRI Scans

Afaf Tareef
Faculty of Information Technology, Mutah University, Jordan
a.tareef@mutah.edu.jo (corresponding author)

Received: 23 September 2024 | Revised: 7 October 2024 and 8 October 2024| Accepted: 9 October 2024

 DOI: https://doi.org/10.48084/etasr.9080

ABSTRACT

Accurate identification of brain tissue is an ill-posed problem due to the inhomogeneous intensity and the extremely complicated and irregular border between endocrine tissues. This study introduces a superpixel-based approach to brain tissue classification in MRI scans. The proposed approach starts with image smoothing and feature highlighting, followed by image splitting based on the SLIC superpixel and merging strategy. Then, distinct superpixel-based appearance and boundary features are extracted and refined by minimizing redundancy and maximizing relevance technique before sending to the C-support vector classifier. Finally, a refinement step is adopted based on morphological characteristics and the distance regularized level set evolution model to modify the matter contour. The proposed approach was evaluated and compared with ten existing algorithms using the publicly accessible IBSR dataset. The experimental results show the better efficiency of the proposed approach in delimiting the contour of each matter than the other approaches in the literature.

Keywords-brain tissue MRI; classification; feature selection; c-support vector classification; distance regularized level set evolution

I. INTRODUCTION

Magnetic Resonance Imaging (MRI) is a popular medical imaging modality that presents important structural data about the brain. Complete and accurate automatic segmentation of MRI brain tissue plays a vital role in a variety of clinical applications, such as disease diagnosis, surgical planning, and treatment monitoring. Over the past years, various unsupervised and supervised classification techniques have been proposed to segment MRI brain images into White Matter (WM), Gray Matter (GM), Cerebrospinal Fluid (CSF), and background.

Unsupervised methods are commonly used for brain tissue segmentation, such as expectation maximization, k-means, and fuzzy clustering. Fuzzy C-Means clustering (FCM) [1] is an unsupervised method that is successfully exploited although ignoring the spatial information. It was later extended into FANTASM which alters the target function with a penalty term depending on the neighbors' membership to other classes, leading to better performance. Fuzzy clustering shows a high capacity to handle complex, largely uncertain, and imprecise brain images. Another FCM-based method was introduced in [2]. This method incorporated a kernel-induced distance, instead of the original Euclidean distance in the FCM, and local spatial information into a weighted membership function. This leads to an improved accuracy compared to the classical FCM.

In [3], a fuzzy consensus clustering technique was presented to classify image pixels based on a voting technique defining a membership function. This algorithm starts with image preprocessing before segmenting the MRI image with common fuzzy and intuitionistic set methods. Then, a voting technique is adopted to combine the results obtained. In [4], another brain segmentation method was introduced, based on pixel- and superpixel-wise features classified with LSTM. Combining these two features enhances computational efficiency and robustness to noise. However, unsupervised clustering methods generally fail in segmenting images with existing noise and intensity heterogeneity resulting from the acquisition procedure.

The Markov Random Field (MRF) model was used in [5, 6]. Specifically, in [4], the iterative expectation maximization technique was integrated with K-means initialization to estimate the MRF parameters, whereas in [6], a real-coded genetic algorithm was employed to estimate the iterative conditional mode algorithm and initialization parameters. The Gaussian mixture model was also used for brain tissue segmentation in SPM5 [7] and SPM8 [8]. SPM5 and SPM8 differ in mixing proportions, registration, and an extended set of probabilistic atlases. Similarly to SPM methods, a Gaussian mixture model was also used in [10] to derive tissue distributions by GAMIXTURE. In this algorithm, a real-coded genetic method was applied to estimate the GMM initial and subsequent parameters.

Semi-supervised and supervised learning algorithms based on training data have also been used for MRI brain tissue segmentation. One such approach was presented in [9] using a Self-Organizing Map (SOM) neural network, where statistical analysis was applied to the extracted features before entering the neural network to organize unknown data into classes based on a similarity criterion, e.g., Euclidean distance. In [11], a

self-trained k-nearest neighbor classifier trained by registering brain atlases was presented to classify objects with the maximum probability group acquired from the tissue atlases.

Recently, machine learning and neural networks have been used for medical image segmentation and classification. A fuzzy min-max neural network was used in [12] for MRI tissue segmentation. This approach starts with image denoising using the Gabor filtering technique, followed by a region-growing technique. The edges were obtained with an edge detection approach on the segmented image. The color information was then abstracted using an entropy-based method after removing the texture information. A comparison of distance in regions was used to merge comparable areas in the region merging stage. Finally, a fuzzy min-max neural network was applied to categorize the regions. Moreover, the maximum-a-posteriori classifier was employed in [13] to combine the partial volume tissue measurement model with spatial prior. Deep networks have also been adopted for supervised MRI brain segmentation [14-16]. For instance, SegNet with an encoder-decoder architecture was introduced in [16]. Besides the acceptable performance of MRI brain tissue segmentation in the literature, most of the existing methods have certain limitations, including requiring predefined parameters for each dataset, high computational complexity, and pixel-wise misclassification.

This study presents a superpixel-based classification approach for MRI brain tissue. The proposed approach incorporates discriminative appearance and boundary cues, sufficiently distinguishing different tissue components at the superpixel representation level. These cues are then used with the trained C-SVC. Then, the Distance Regularized Level Set Evolution (DRLSE) model is adopted for the classified regions to obtain a more accurate border. The proposed approach is compared with ten classification approaches, showing higher performance in CSF, GM, and WM classification.

II. RESEARCH METHODOLOGY

The proposed model was used on a publicly available Internet Brain Segmentation Repository (IBSR) dataset [17], which consists of 20 MRI brain images, each with several subjects with a size of 256×256 pixels. These images were preprocessed, classified, and post-processed as shown in Figure 1. The proposed model consists of three main phases: 1) MRI brain preprocessing and superpixelling phase, 2) C-support vector classification with superpixel-based distinctive features, and 3) MRI brain matter refinement phase based on edge and shape.

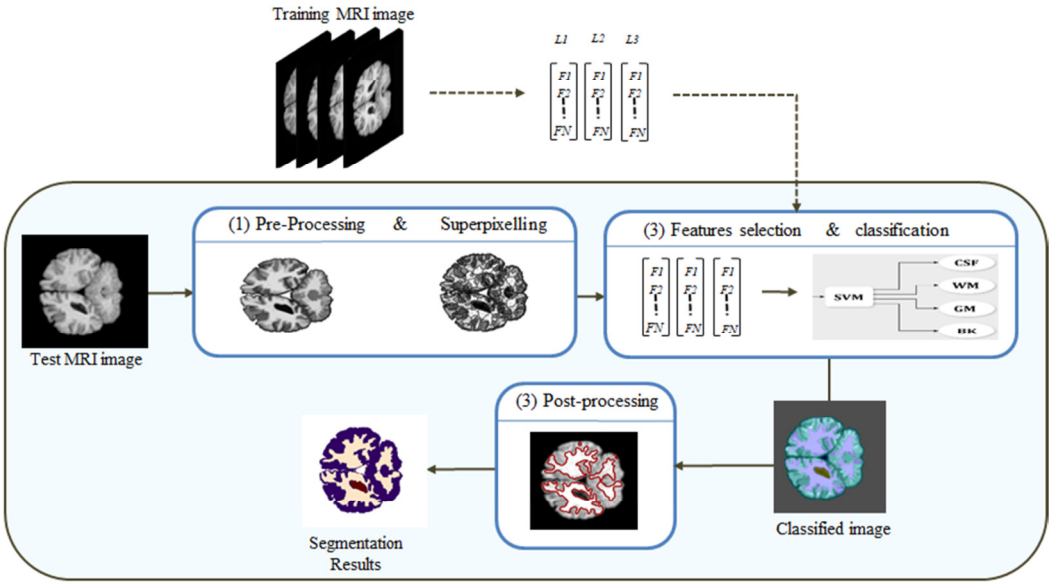

Fig. 1. The flowchart of the proposed approach: (1) Preprocessing and superpixelling phase, (2) feature extraction and classification phase, and (3) post-processing phase by shape and edge-based refinement.

A. *Preprocessing and Superpixelling Phase*

The preprocessing phase plays a vital role in the accurate classification of MRI tissue and consists of several steps:

- Intensity normalization: Intensity is one of the most dominant and recognizable low-level visual characteristics to describe a CSF region in an MRI brain image. However, it varies based on the difference between the acquisitions of various sequences. Thus, intensity normalization is performed to enhance the appearance of brain tissue.
- Image smoothing: Smoothing is accomplished using the Gabor filtering technique to enhance the image texture and eliminate the noise, thus, the brain matters will be accurately classified in the next phase.
- Feature highlighting: For this purpose, Contrast-Limited Adaptive Histogram Equalization (CLAHE) [18] and morphological filtering by reconstruction (opening and closing) [19] were used to highlight the discriminative characteristics of brain tissue.

- SLIC superpixelling: The MRI data is divided into small regions with similar color information using the Simple Linear Iterative Clustering Technique (SLIC) [20]. SLIC is one the most efficient superpixelling techniques and is widely used with medical images due to its low computational time and ability to produce regularly shaped and semi-equal-sized superpixels, facilitating the differentiation of image components based on the superpixel shape. It performs in a five-dimensional color and image plane space, efficiently producing condensed and nearly homogenous superpixels by incorporating color and spatial information [21].
- Superpixel fusion: Superpixelling may produce some small superpixels with few isolated pixels, which may lead to misclassifying them later. Thus, a fusion step is performed to integrate superpixels smaller than 50 pixels with their adjacent superpixels. All background superpixels are merged into a single superpixel as well.

B. *Superpixel-based Classification Phase*

The classification phase is then performed to divide the MRI brain image into CSF, gray, and white matters, as shown in Figure 2. This is performed in two steps:

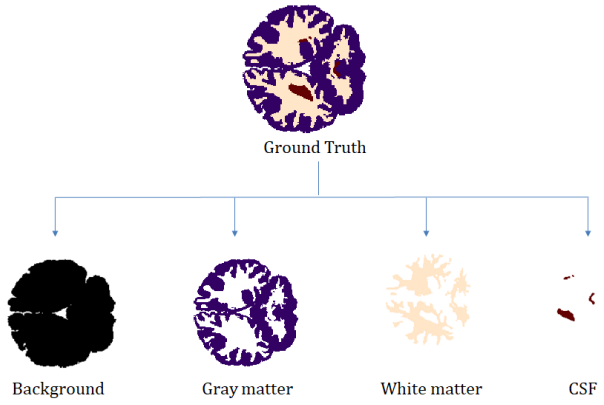

Fig. 2. The components of an MRI brain tissue image.

- Feature selection: First, distinct features are extracted from each superpixel for subsequent classification. According to our observation, the CSF region can be distinguished by dark and smooth intensity, elliptical shape, and connected edge surrounding the region. Thus, a set of texture, edge, and shape features, as well as comparative features with good discriminative ability are extracted from each superpixel including, average and median intensity, standard deviation, entropy, the average intensity difference between the patch-in-focus and the surrounding patches, number of border pixels, area, and circularity. The extracted features are then refined using the minimum Redundancy Maximal Relevance (mRMR) feature selection algorithm [22] to choose the most suited features to distinguish brain tissue based on the maximal statistical dependency criterion of mutual information.
- Superpixel classification: For this purpose, a C-Support Vector Classifier (C-SVC) was used to classify the superpixels into MRI components using the selected superpixel-based features by the mRMR algorithm. A C-SVC from the LIBSVM package [23] was used. The C-SVC method was trained using the labeled superpixels from the training MRI brain images. C-SVC has shown effectiveness in addressing many challenging classification and segmentation problems in medical images [24].

C. *Shape and Edge-based Refinement Phase*

This phase aims to correct the misclassification of some dark tissue pixels as background or CSF, using the following steps:

- Shape-based refinement: This step starts with identifying the pixels located between the classified brain matters and the image background obtained by triangle thresholding [25], and labeling those pixels as gray matters. Then, the morphological shape characteristics of the classified matters are used to filter the regions that are smaller than the corresponding matter. In addition, the potential CSF regions are checked in terms of size and circularity, and the misclassified CSF regions are labeled GM.
- Edge-based refinement: Finally, edge-based refinement is performed to define the accurate segmentation of the MRI tissue matters and eliminate extra pixels at the matter border. For this purpose, the DRLSE model [26] was adopted. To retain the desired form of the level set function, a distance regularization term was developed with a potential function giving the level set evolution a special forward-and-backward diffusion effect. DRLSE ensures curve smoothness and does away with the necessity for the time-consuming re-initialization process by forcing the curve to develop around the signed distance function. Assume that the symbol ϕ signifies a level set function on a Ω domain. The energy functional to be reduced is given as follows:

$$\varepsilon = c_1 R(\phi) + c_2(L)(\phi) + c_3 A(\phi) \quad (1)$$

where c_1, c_2, and c_3 are constants, $R(\phi)$ is a regularization term that keeps the signed distance condition $\nabla\phi = 1$ to ensure smoothness, and $L(\phi)$ and $A(\phi)$ measure the length and area of the zero level, respectively. By resolving the gradient flow, it is possible to minimize the energy functional $\varepsilon(\phi)$ as follows:

$$\frac{\partial\phi}{\partial t} = c_1 div\,(d_p(|\nabla\phi|\nabla\phi) + c_2\delta_\epsilon(\phi) div\left(S\frac{\nabla\phi}{|\nabla\phi|}\right) + c_3 S\delta_\epsilon(\phi) \quad (2)$$

where $\delta(.)$is the Dirac delta function, and S is the edge-stopping function adopted to stop the evolving contour at the region boundaries, computed as follows:

$$S(|\nabla f|) = \frac{1}{1+|\nabla\sigma \times f|^2}$$

where σ is the Gaussian kernel, and f is the image on a domain Ω.

III. EXPERIMENTAL RESULTS

The Dice similarity coefficient [27] was calculated to measure the overlap between the classified regions and the ground-truth regions. DSC is calculated as follows:

$$DSC = 2\frac{|R_{GT} \cap R_{Seg}|}{|R_{GT}| + |R_{Seg}|} \quad (4)$$

where R_{GT} and R_{Seg} are the ground truth and classified matters, respectively, and $|.|$ denotes the number of pixels in the region. DSC has a range of 0 to 1, with a higher value indicating better performance. Unlike other measures (e.g., Sensitivity, Specificity, False Negative, and False Positive Rates), DSC incorporates positive and negative outcomes, giving a better representation of overall similarity and differences between the ground truth and classified regions [28].

The performance of the proposed approach was compared with ten brain tissue classification approaches on the same dataset. The comparison includes five unsupervised methods, i.e., FCM [1], FAST [5], SPM5 [7], SPM8 [8], GAMIXTURE [10], and five supervised classification methods, i.e., SOM [9], KNN [11], FANTASM [30], PVC [13], SegNet [16]. Tables I and II present the comparison results in terms of DSC mean and standard deviation. The results show that most other approaches failed to classify CSF. In [30], this was justified by the misclassification of the Sulcal Cerebrospinal Fluid (SCSF) as CSF or background regions instead of GM. Therefore, it is suggested to evaluate classification performance by ignoring the SCSF regions. Thus, the performance of the proposed and other approaches was evaluated and presented in the two cases, i.e., the normal case with the original ground truth annotations in Table I, and the second, by ignoring the SCSF regions in Table II. The highest value is shown in bold.

According to Table I, the proposed approach achieved the best classification performance for all tissue regions, i.e., WM, GM, and CSF in the case of considering SCSF regions. The proposed method obtained a DSC of 0.80 for GM, 0.82 for WM, and 0.66 for CSF classification. Table II shows that the performance of the proposed approach in GM and WM classification was improved to 0.87 and 0.82, respectively, when ignoring the SCSF regions. Moreover, the proposed scheme obtains a lower standard deviation than the other methods.

TABLE I. COMPARISON IN TERMS OF DSC ± STANDARD DEVIATION USING THE ORIGINAL GROUND TRUTH ANNOTATIONS

Methods	GM	WM	CSF
FCM	0.70 ± 0.09	0.78 ± 0.14	0.15 ± 0.05
FAST	0.69 ± 0.06	0.80 ± 0.10	0.14 ± 0.04
SPM5	0.77 ± 0.06	0.81 ± 0.04	0.18 ± 0.07
SPM8	0.79 ± 0.06	0.82 ± 0.08	0.22 ± 0.07
GAMIXTURE	0.78 ± 0.09	0.75 ± 0.16	0.26 ± 0.12
SOM	0.70 ± 0.09	0.78 ± 0.14	0.16 ± 0.06
KNN	0.65 ± 0.09	0.81 ± 0.06	0.14 ± 0.04
FANTASM	0.71 ± 0.10	0.78 ± 0.14	0.16 ± 0.06
PVC	0.67 ± 0.11	0.64 ± 0.23	0.14 ± 0.05
SegNet	0.74 ± 0.07	0.71 ± 0.04	0.65 ± 0.08
Proposed Model	**0.80 ± 0.03**	**0.82 ± 0.03**	**0.66 ± 0.20**

TABLE II. COMPARISON TERMS OF DSC ± STANDARD DEVIATION WITH IGNORING THE SCSF REGIONS.

Methods	GM	WM	CSF
FCM	0.82 ± 0.08	0.78 ± 0.14	0.77 ± 0.12
FAST	0.83 ± 0.06	0.79 ± 0.12	0.77 ± 0.12
SPM5	0.87 ± 0.03	0.83 ± 0.02v	0.83 ± 0.08
SPM8	0.87 ± 0.06	0.82 ± 0.07	**0.84± 0.08**
GAMIXTURE	0.84 ± 0.06	0.75 ± 0.16	0.76 ± 0.10
SOM	0.82 ± 0.08	0.78 ± 0.14	0.77 ± 0.12
KNN	0.79 ± 0.08	0.81 ± 0.06	0.76 ± 0.12
FANTASM	0.82 ± 0.08	0.78 ± 0.14	0.78 ± 0.12
PVC	0.80 ± 0.09	0.53 ± 0.24	0.78 ± 0.12
SegNet	0.74 ± 0.07	0.71 ± 0.04	0.65 ± 0.08
Proposed Model	**0.87 ± 0.02**	**0.82 ± 0.03**	0.66 ± 0.19

Figure 3 illustrates the visual inspection of the classification performance of the proposed method compared to the performance of the unsupervised classification in [1] and the supervised classification in [9]. The proposed method had the best classification performance similar to the ground truth, whereas the other two methods fail in classifying the GM and CSF regions.

Overall, the proposed method yielded superior performance compared to other methods. This superior performance returns the superpixel-based features successfully representing the different brain regions. For example, CSF regions are characterized by comparatively low and homogeneous appearance with well-defined semicircular shapes, which are properly represented by the extracted intensity, edge, and shape features. In addition, the feature selection algorithm helps in filtering these features to select the best features based on the training dataset, leading to more accurate classification.

IV. CONCLUSIONS

Accurate automated segmentation of brain tissue plays a significant role in the clinical diagnosis of brain diseases using MRI. This study proposed an efficient superpixel-based classification model for MRI brain tissue. The proposed model is based on a C-SVC trained on robust intensity, boundary, and shape features, as well as comparative features with good discriminative ability. The selected features successfully represent the difference between the brain regions, leading to high classification accuracy. Moreover, a post-processing procedure is utilized, including matter filtering and regularization based on morphological features and the DRLSE model to further improve the pixel-wise classification performance.

The proposed technique was evaluated and compared with ten supervised and unsupervised classification techniques using ISRB20 images. The comparison results demonstrate the superiority of the proposed approach in classifying all brain tissue components, i.e., GM, WM, and CSF matters. The proposed model yields a DSC value above 0.8 for GM, 0.82 for WM, and 0.66 for CSF, with 11%, 7%, and 200% performance improvements over the existing approaches, respectively. Quantitative and qualitative evaluations show a good improvement over other classification techniques. Future studies should integrate more effective and discriminative features with classifiers to improve the segmentation of MRI brain images or to detect tumors on pathological images.

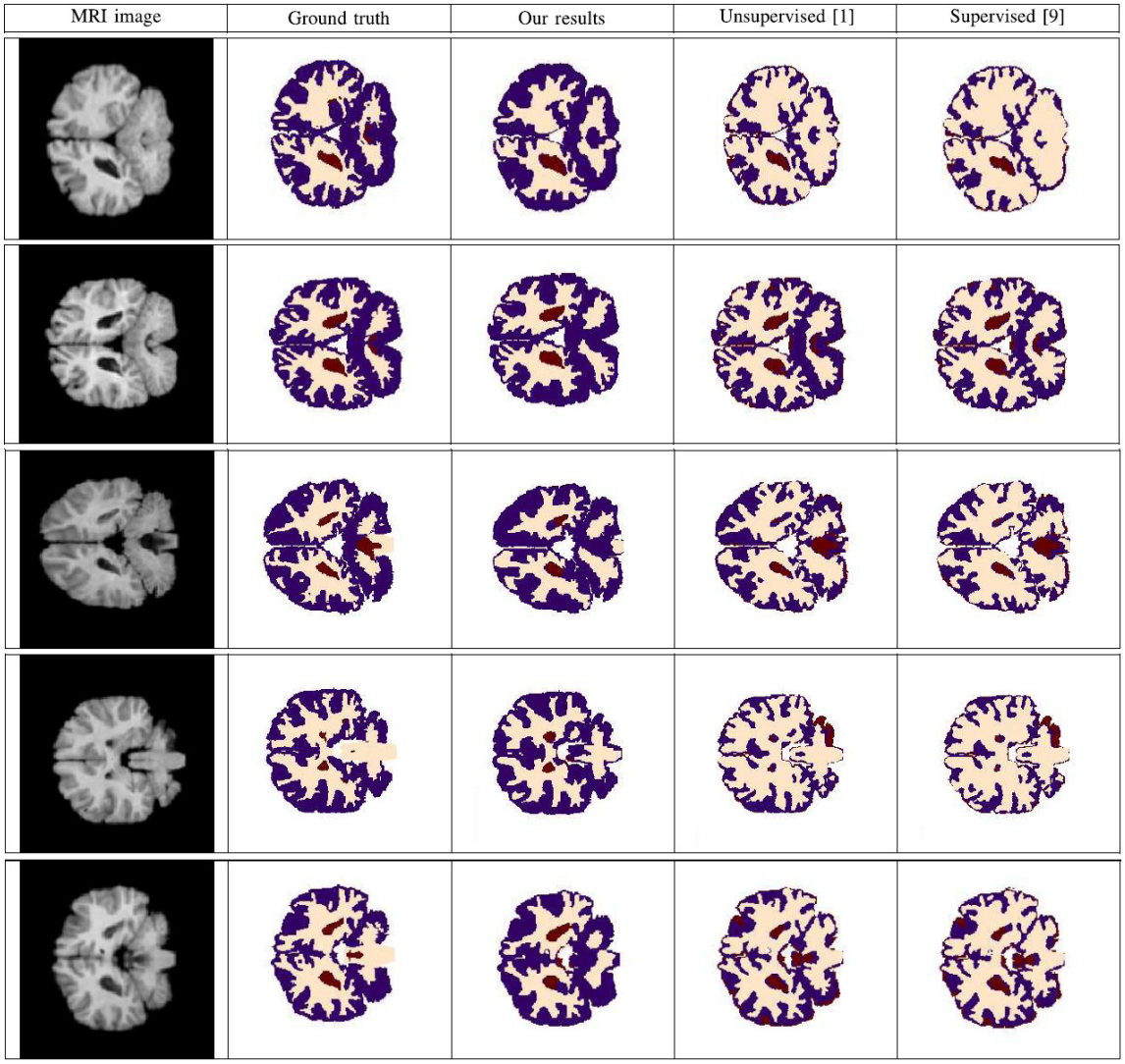

Fig. 3. Randomly chosen test samples from the IBSR dataset, where the first column represents the original MRI brain images, the second column represents the ground-truth tissue maps, the third column represents the predicted tissue maps of the proposed approach, and the fourth and fifth columns represent the predicted tissue maps of unsupervised clustering [1] and the predicted tissue maps of supervised clustering [9], respectively

REFERENCES

[1] D. L. Pham, "Spatial Models for Fuzzy Clustering," *Computer Vision and Image Understanding*, vol. 84, no. 2, pp. 285–297, Nov. 2001, https://doi.org/10.1006/cviu.2001.0951.

[2] B. Gharnali and S. Alipour, "MRI Image Segmentation Using Conditional Spatial FCM Based on Kernel-Induced Distance Measure," *Engineering, Technology & Applied Science Research*, vol. 8, no. 3, pp. 2985–2990, Jun. 2018, https://doi.org/10.48084/etasr.1999.

[3] S. V. Aruna Kumar, E. Yaghoubi, and H. Proença, "A Fuzzy Consensus Clustering Algorithm for MRI Brain Tissue Segmentation," *Applied Sciences*, vol. 12, no. 15, Jan. 2022, Art. no. 7385, https://doi.org/10.3390/app12157385.

[4] K. Xie and Y. Wen, "LSTM-MA: A LSTM Method with Multi-Modality and Adjacency Constraint for Brain Image Segmentation," in *2019 IEEE International Conference on Image Processing (ICIP)*, Taipei, Taiwan, Sep. 2019, pp. 240–244, https://doi.org/10.1109/ICIP.2019.8802959.

[5] Y. Zhang, M. Brady, and S. Smith, "Segmentation of brain MR images through a hidden Markov random field model and the expectation-maximization algorithm," *IEEE Transactions on Medical Imaging*, vol. 20, no. 1, pp. 45–57, Jan. 2001, https://doi.org/10.1109/42.906424.

[6] J. Tohka, I. D. Dinov, D. W. Shattuck, and A. W. Toga, "Brain MRI tissue classification based on local Markov random fields," *Magnetic Resonance Imaging*, vol. 28, no. 4, pp. 557–573, May 2010, https://doi.org/10.1016/j.mri.2009.12.012.

[7] J. Ashburner and K. J. Friston, "Unified segmentation," *NeuroImage*, vol. 26, no. 3, pp. 839–851, Jul. 2005, https://doi.org/10.1016/j.neuroimage.2005.02.018.

[8] J. Ashburner *et al.*, "SPM8 Manual," Institute of Neurology, London, UK, Feb. 2012.

[9] J. Tohka *et al.*, "Genetic Algorithms for Finite Mixture Model Based Voxel Classification in Neuroimaging," *IEEE Transactions on Medical Imaging*, vol. 26, no. 5, pp. 696–711, Feb. 2007, https://doi.org/10.1109/TMI.2007.895453.

[10] D. Tian and L. Fan, "A Brain MR Images Segmentation Method Based on SOM Neural Network," in *2007 1st International Conference on Bioinformatics and Biomedical Engineering*, Wuhan, China, 2007, pp. 686–689, https://doi.org/10.1109/ICBBE.2007.179.

[11] R. de Boer *et al.*, "White matter lesion extension to automatic brain tissue segmentation on MRI," *NeuroImage*, vol. 45, no. 4, pp. 1151–1161, May 2009, https://doi.org/10.1016/j.neuroimage.2009.01.011.

[12] S. L. Bangare, "Classification of optimal brain tissue using dynamic region growing and fuzzy min-max neural network in brain magnetic resonance images," *Neuroscience Informatics*, vol. 2, no. 3, Sep. 2022, Art. no. 100019, https://doi.org/10.1016/j.neuri.2021.100019.

[13] D. W. Shattuck, S. R. Sandor-Leahy, K. A. Schaper, D. A. Rottenberg, and R. M. Leahy, "Magnetic Resonance Image Tissue Classification Using a Partial Volume Model," *NeuroImage*, vol. 13, no. 5, pp. 856–876, May 2001, https://doi.org/10.1006/nimg.2000.0730.

[14] H. Allioui, M. Sadgal, and A. Elfazziki, "Deep MRI Segmentation: A Convolutional Method Applied to Alzheimer Disease Detection," *International Journal of Advanced Computer Science and Applications*, vol. 10, no. 11, pp. 365–371, 2019, https://doi.org/10.14569/IJACSA.2019.0101151.

[15] A. Jijja and Dr. Dinesh, "Efficient MRI Segmentation and Detection of Brain Tumor using Convolutional Neural Network," *International Journal of Advanced Computer Science and Applications*, vol. 10, no. 4, 2019, https://doi.org/10.14569/IJACSA.2019.0100466.

[16] B. Khagi and G. R. Kwon, "Pixel-Label-Based Segmentation of Cross-Sectional Brain MRI Using Simplified SegNet Architecture-Based CNN," *Journal of Healthcare Engineering*, vol. 2018, no. 1, 2018, Art. no. 3640705, https://doi.org/10.1155/2018/3640705.

[17] "Internet Brain Segmentation Repository (IBSR)." http://www.cma.mgh.harvard.edu/ibsr.

[18] K. Zuiderveld, "Contrast limited adaptive histogram equalization," in *Graphics gems IV*, USA: Academic Press Professional, Inc., 1994, pp. 474–485.

[19] P. Maragos and R. Schafer, "Morphological filters–Part I: Their set-theoretic analysis and relations to linear shift-invariant filters," *IEEE Transactions on Acoustics, Speech, and Signal Processing*, vol. 35, no. 8, pp. 1153–1169, Aug. 1987, https://doi.org/10.1109/TASSP.1987.1165259.

[20] R. Achanta, A. Shaji, K. Smith, A. Lucchi, P. Fua, and S. Süsstrunk, "SLIC Superpixels," EPFL Technical Report 149300, Jun. 2010.

[21] U. Diaa, "A Deep Learning Model to Inspect Image Forgery on SURF Keypoints of SLIC Segmented Regions," *Engineering, Technology & Applied Science Research*, vol. 14, no. 1, pp. 12549–12555, Feb. 2024, https://doi.org/10.48084/etasr.6622.

[22] H. Peng, F. Long, and C. Ding, "Feature selection based on mutual information criteria of max-dependency, max-relevance, and min-redundancy," *IEEE Transactions on Pattern Analysis and Machine Intelligence*, vol. 27, no. 8, pp. 1226–1238, Dec. 2005, https://doi.org/10.1109/TPAMI.2005.159.

[23] C. C. Chang and C. J. Lin, "LIBSVM: A library for support vector machines," *ACM Transactions on Intelligent Systems and Technology*, vol. 2, no. 3, pp. 1–27, Apr. 2011, https://doi.org/10.1145/1961189.1961199.

[24] D. Gupta, "A Hybrid Technique Based on Fuzzy Methods and Support Vector Machine for prediction of Brain Tumor," *International Journal on Computer Science and Engineering*, vol. 9, no. 8, pp. 517–521, Aug. 2017.

[25] G. W. Zack, W. E. Rogers, and S. A. Latt, "Automatic measurement of sister chromatid exchange frequency.," *Journal of Histochemistry & Cytochemistry*, vol. 25, no. 7, pp. 741–753, Jul. 1977, https://doi.org/10.1177/25.7.70454.

[26] C. Li, C. Xu, C. Gui, and M. D. Fox, "Distance Regularized Level Set Evolution and Its Application to Image Segmentation," *IEEE Transactions on Image Processing*, vol. 19, no. 12, pp. 3243–3254, Sep. 2010, https://doi.org/10.1109/TIP.2010.2069690.

[27] L. R. Dice, "Measures of the Amount of Ecologic Association Between Species," *Ecology*, vol. 26, no. 3, pp. 297–302, 1945, https://doi.org/10.2307/1932409.

[28] A. P. Zijdenbos, B. M. Dawant, R. A. Margolin, and A. C. Palmer, "Morphometric analysis of white matter lesions in MR images: method and validation," *IEEE Transactions on Medical Imaging*, vol. 13, no. 4, pp. 716–724, Sep. 1994, https://doi.org/10.1109/42.363096.

[29] D. L. Pham, "Robust fuzzy segmentation of magnetic resonance images," in *Proceedings 14th IEEE Symposium on Computer-Based Medical Systems. CBMS 2001*, Bethesda, MD, USA, 2001, pp. 127–131, https://doi.org/10.1109/CBMS.2001.941709.

[30] S. Valverde, A. Oliver, M. Cabezas, E. Roura, and X. Lladó, "Comparison of 10 brain tissue segmentation methods using revisited IBSR annotations," *Journal of Magnetic Resonance Imaging*, vol. 41, no. 1, pp. 93–101, 2015, https://doi.org/10.1002/jmri.24517.

AUTHORS PROFILE

Afaf Tareef received a B.Sc. degree in computer science from Mutah University, Jordan in 2008, an M.Phil. degree from the University of Jordan in 2010, and a Ph.D. degree from the University of Sydney, Australia in 2017. She is currently an Associate Professor in the Faculty of Information Technology at Mutah University, Jordan. She has many publications in several international conferences and journals. Her research interests include image processing and medical image analysis.